Quantum Electronics **40** (6) 471–474 (2010)

LASERS

PACS numbers: 42.55.Rz; 42.55.Xi; 42.60.Fc; 42.62.Fi
DOI: 10.1070/QE2010v040n06ABEH014345

Diode-pumped tunable Tm:YLF laser for mid-infrared gas spectroscopy

O.N. Eremeykin, A.P. Savikin, K.Yu. Pavlenko, V.V. Sharkov

Abstract. **The spectral characteristics of the longitudinally diode-pumped Tm:YLF laser radiation are experimentally studied. The laser wavelength was tuned within a spectral range of 1860–1940 nm with a linewidth not exceeding 1 nm. The effect of water vapour on the spectral characteristics is studied.**

Keywords: *Tm : YLF laser, diode pumping, intracavity spectroscopy of water vapour.*

1. Introduction

The remote absorption and/or scattering spectroscopy of molecular gases is one of the most important applied problems, which is solved using mid-IR sources. To design compact and efficient laser systems operating in the mid-IR region, one uses lasers based on crystals doped with Tm^{3+} ions. In particular, Tm:YLF lasers pumped at 790–795 nm emit high-power radiation at a wavelength of 1908 nm with a high beam quality and a high pump conversion efficiency [1–3]. In order to extend the available spectral region, one can use Tm:YLF lasers to pump Ho:YAG crystals emitting at a wavelength of 2.1 μm, which in the future will allow one to obtain radiation in the region of 3–5 μm with the use of optical parametric oscillators [4, 5].

The Tm:YLF lasers seem to be promising as optical pump sources for chalcogenide crystals (ZnS, ZnSe, CdSe, and others) doped with ions of transition metals (Cr, Co, Ni, Fe, etc.). This will provide the possibility of creating compact and efficient lasers tunable within the wavelength range of 2–5 μm for gas spectroscopy, including high-sensitive intracavity laser spectroscopy [6–9].

Since the Tm:YLF laser spectrum lies in the region of vibrational–rotational absorption transitions of water molecules, it is always affected by the water vapours contained in the atmosphere [1]. The use of selective cavities makes it possible to control the width and position of the laser spectrum and, thus, to detune from the water vapour absorption lines.

In this work, we experimentally studied the spectral characteristics of a longitudinally diode-pumped Tm:YLF laser using an interference-polarisation filter. We studied the effect of water vapour on the spectrum of a laser placed inside a chamber, which could be pumped with nitrogen.

2. Experimental setup

The cavity of the laser under study consisted of a plane highly reflecting mirror (*1*) and a spherical output mirror (*2*) with the radius of curvature of 200 mm and transmittance $T \approx 11\%$ at the lasing wavelength; the cavity length L_r was 120 mm (Fig. 1). A Tm:YLF crystal (*3*) (Tm^{3+} concentration of about 2.5 wt%, length 18 mm, diameter 3 mm) was held in a copper heat sink at a stable temperature of 15 °C and pumped by the 793-nm radiation of Coherent FAP-800 diode arrays with pigtails (*4*). The pump radiation was coupled into the cavity through dichroic mirrors (*5*) with a high reflectance at the pump wavelength; a system of lenses (*6*) transferred the 1:1 image from the end of fibre pigtails (*4*) to the Tm:YLF crystal.

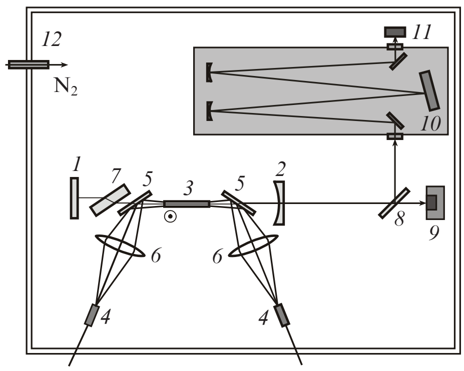

Figure 1. Scheme of the experimental setup: (*1*) highly reflecting mirror; (*2*) output mirror; (*3*) Tm:YLF crystal; (*4*) fibre pigtails of the pump diode lasers; (*5*) dichroic mirrors; (*6*) optical condensers; (*7*) phase plate; (*8*) semitransparent mirror; (*9*) power meter; (*10*) MDR-41 spectrograph; (*11*) FSA-G1 photodetector; (*12*) nitrogen-pumped chamber.

Tm:YLF is a uniaxial anisotropic crystal with intense broad emission bands in the spectral region of 1.75–1.95 μm with π and σ polarisations (Fig. 2). To achieve lasing at a wavelength of 1908 nm, the optical axis of the crystal was oriented perpendicular to the scheme plane. The dichroic mirror had the minimum losses for the desired σ polarisation. For tuning the laser radiation spectrum, we placed inside the

O.N. Eremeykin Institute of Applied Physics, Russian Academy of Sciences, ul. Ul'yanova 46, 603950 Nyzhnii Novgorod, Russia; N.I. Lobachevskii State University of Nizhnii Novgorod, prosp. Gagarina 23, 603950 Nyzhnii Novgorod, Russia; e-mail: eon@rambler.ru;
A.P. Savikin, K.Yu. Pavlenko, V.V. Sharkov N.I. Lobachevskii Nizhnii Novgorod State University, prosp. Gagarina 23, 603950 Nyzhnii Novgorod, Russia; e-mail: savikin@rf.unn.ru

Received 5 February 2010; revision received 16 April 2010
Kvantovaya Elektronika **40** (6) 471–474 (2010)
Translated by M.N. Basieva

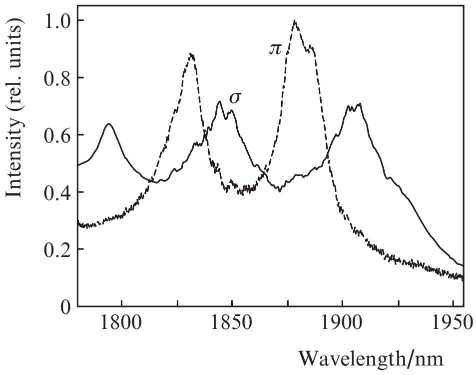

Figure 2. Luminescence spectrum of a Tm:YLF crystal (spectral resolution $\delta\lambda \sim 1$ nm).

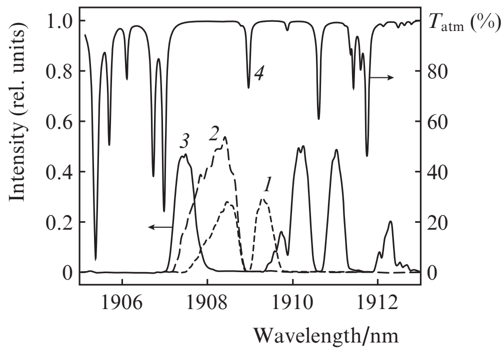

Figure 4. Spectra of the Tm:YLF laser at the output power $P_{gen} = 1.2$ (*1*), 4 (*2*) and 6 W (*3*) and the transmission spectrum of one meter of the standard atmosphere T_{atm} (*4*) [10].

cavity a sapphire phase plate (*7*) 5 mm thick mounted on a motorised rotary table (Standa, minimum step 1/200°).

The Tm:YLF laser spectrum was measured by an MDR-41 spectrograph with the minimum spectral resolution $\delta\lambda \sim 0.1$ nm in the wavelength region 1.8–2 μm. The radiation was recorded by an FSA-G1 PbS photoresistor placed at the exit slit of the spectrograph. The remote control of the spectrograph and rotary table (with the phase plate) motors and of the diode array current source, as well as the data accumulation and processing, were performed using a computer system based on an NI_PCI_6251 card; the program of the control and of the data processing and graphic display was written in the LabVIEW software environment.

The laser and recording system were placed inside a hermetic nitrogen-pumped chamber (Fig. 1), which allowed us to change the water vapour concentration. The humidity inside the chamber was measured with a portable digital CENTER 310 humidity meter.

3. Operation of a Tm:YLF laser with a nonselective cavity

In the described scheme, we obtained lasing with a slope efficiency of about 32% and the beam quality factor $M^2 \leqslant 2.5$ (Fig. 3). The radiation was horizontally polarised, the polarisation ellipticity (no less than 1:200) being determined by the polarising properties of the dichroic mirrors and by the Tm:YLF crystal anisotropy. We obtained spiking-mode lasing with a spike-repetition period of 30–50 μs; the individual spike duration was ~5 μs at the output power of 2 W.

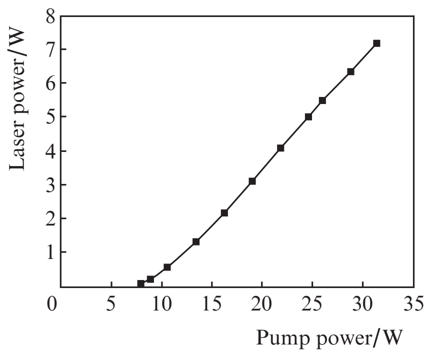

Figure 3. Dependence of the laser output power on the pump power.

The shape and position of the laser spectrum depended on the pump power (Fig. 4). At the near-threshold pump powers, the spectrum lies in the region of 1908.5 nm; with increasing power, the spectrum dynamics has a complicated character, namely, it smoothly shifts, extends, and changes in shape. This behaviour can be explained both by the dependence of the gain spectrum on the pump power and by the temperature dependence of losses caused by the absorption at the laser transition.

The laser spectrum shows holes near wavelengths of 1909, 1910, 1910.5 and 1911.5 nm. This allowed us to suggest the existence of high intracavity losses caused by the absorption of radiation in the atmosphere. Indeed, the holes in the Tm:YLF laser spectrum coincide with the water vapour absorption lines (Fig. 4, Table 1) [1, 10]. The depth of the spectral holes was observed to decrease as the humidity

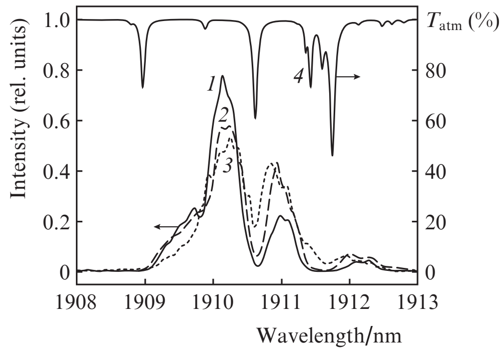

Figure 5. Spectra of the Tm:YLF laser at the relative air humidity $\varphi = 23\%$ (*1*), 9% (*2*) and 2% (*3*) and the transmission spectrum of one meter of the standard atmosphere T_{atm} (*4*) [10] ($P_{gen} = 7.5$ W).

Table 1. Most intense absorption lines of water in the spectral region 1905–1914 nm [10].

Transition	Wavelength /nm	Absorption cross section/cm^2	Linewidth /cm^{-1}
011–000	1913.76	1.56×10^{-20}	0.087
	1911.75	5.06×10^{-21}	0.090
	1910.61	3.27×10^{-21}	0.087
	1906.98	8.78×10^{-21}	0.085
	1906.73	6.76×10^{-21}	0.091
	1905.38	1.94×10^{-20}	0.091
	1903.02	1.77×10^{-20}	0.094
110–000	1908.97	1.94×10^{-21}	0.085

decreased to 2%. This indicates that the effect of water vapour on the spectral characteristics in this case was weaker due to smaller intracavity losses (Fig. 5).

4. Operation of the Tm : YLF laser with a phase plate inside the cavity

The laser spectrum was controlled by a sapphire plate with the thickness $d = 5$ mm, which was cut parallel to the optical axis of the crystal and placed inside the cavity at the Brewster angle.

The phase shift $\Delta\varphi$ between the ordinary and extraordinary waves propagating through the phase plate, which is determined by the wavelength λ, the refractive indices n_o and n_e, and the thickness d, leads to a change in the polarisation at the plate exit [11]. If $\Delta\varphi = 2\pi n$, where n is an integer number, the initial polarisation of radiation at this wavelength does not change. The laser spectrum was changed by rotating the phase plate around the normal to its surface, since the refractive index n_e for the extraordinary wave depends on the angle θ between the optical axis and the polarisation vector of the incident radiation.

The polarisation-selective losses were determined by the dichroic mirrors, the Tm : YLF crystal anisotropy, and the Brewster faces of the phase plate.

At the Tm : YLF laser wavelength (1908 nm), we experimentally studied the angular dependence of the transmittance T_{sap} of the sapphire phase plate placed outside the cavity at the Brewster angle (the measured period was $\sim$12°) (Fig. 6).

The free dispersion region of an interference-polarisation filter based on a phase plate is

$$\Delta\lambda = \frac{\lambda^2}{d(n_e - n_o)}. \quad (1)$$

For our sapphire phase plate oriented at the Brewster angle ($\lambda = 1908$ nm, $n_e = 1.731$, $n_o = 1.739$), we have $\Delta\lambda \approx 75$ nm. Taking into account that the measured angular period of the phase plate transmittance is about 12%, we find the laser wavelength tuning coefficient of about 6 nm deg^{-1}.

The use of a phase plate inside the cavity allowed us to tune the laser spectrum within a band wider than 70 nm, while the power in the tuning curve maximum decreased no more than by 1.5% (Fig. 7). The angular period of the laser spectrum variation also was 12°, and the tuning coefficient corresponded to the above-estimated value. In the case of detuning from the water vapour absorption line, the linewidth of the laser with the selective cavity was found to be $\delta\lambda_{gen} \leqslant 1$ nm (Fig. 8).

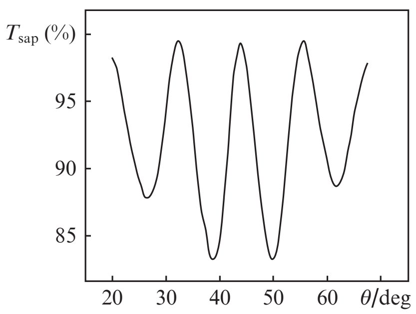

Figure 6. Dependence of the transmittance T_{sap} of a sapphire plate placed outside the cavity on the rotation angle θ.

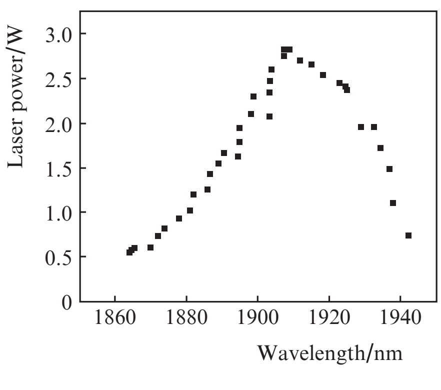

Figure 7. Tuning curve of the Tm : YLF laser with a phase plate at the pump power $P_p = 18$ W.

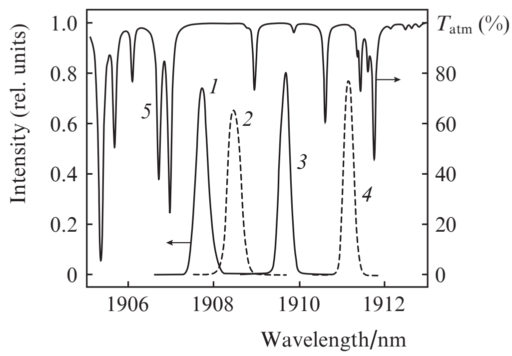

Figure 8. Spectra of the Tm : YLF laser with a phase plate rotated by $\Delta\theta = 0$ (*1*), 0.15° (*2*), 0.35° (*3*) and 0.55° (*4*) and the transmission spectrum of one meter of the standard atmosphere T_{atm} (*5*) [10] ($P_{gen} = 2.2$ W).

The tuning of the selective cavity to one of the water vapour absorption lines resulted in a broadened laser spectrum with a spectral hole in the centre (Fig. 9). As humidity was increased to 2%, the depth of the spectral hole at the wavelength 1908.9 nm decreased, but the more intense lines of water vapour absorption (at 1906.7 and 1907 nm) still completely burned the laser spectrum (Fig. 10).

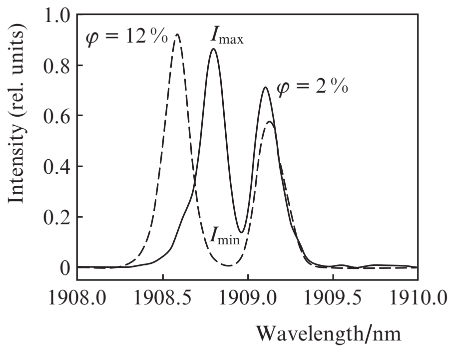

Figure 9. Spectra of the Tm : YLF laser with a phase plate in the case of tuning to the water vapour line 1908.9 nm for the relative humidity $\varphi = 12\%$ and 2%; $P_{gen} = 2.2$ W, $P_p = 16$ W, and the threshold pump power $P_p^{th} = 8$ W.

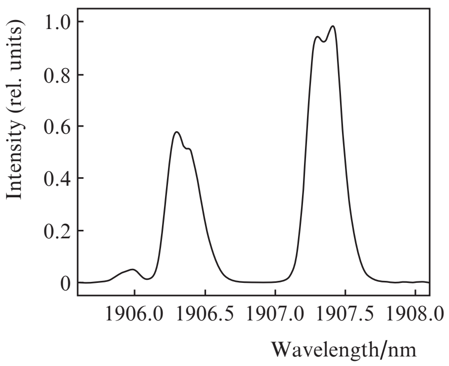

Figure 10. Spectra of the Tm:YLF laser with a phase plate in the case of tuning to the water vapour lines 1906.7 and 1907 nm for the relative humidity $\varphi = 2\%$; $P_{gen} = 2.2$ W, $P_p = 16$ W, and the threshold pump power $P_p^{th} = 8$ W.

5. Discussion of results

In essence, the experimental setup was a broadband version of an intracavity laser spectrometer, whose absorbing cell was the free space of the cavity.

The absorption spectrum of water molecules in the near IR region consists of individual vibrational–rotational lines with homogeneous collision-broadened profiles. At the atmospheric pressure, the width of the observed water vapour absorption lines is $\Delta\lambda_{atm} \sim 0.05$ nm [10, 12], which is twice as low as the width of the instrumental function of the spectrometer used in the experiment. The measured hole in the lasing spectrum is the integral of the convolution of the instrumental function and the real absorption linewidth, which decreases the setup sensitivity [12]. Note that the intermode interval of the cavity is $\Delta\lambda_r \sim 0.015$ nm, i.e., only several longitudinal modes of the cavity fall into the absorption line.

Let us estimate the sensitivity of water vapour detection by the 1908.97-nm line (see Table 1). Since we measured the relative air humidity φ, the volume concentration of water vapour N (in cm^{-3}) was determined by the relation

$$N = 6.02 \times 10^{23} \varphi \frac{\rho_{max}}{M_{H_2O}}, \qquad (2)$$

where ρ_{max} is the maximum humidity of water vapour at the given air temperature (taken from tabular data) and M_{H_2O} is the molecular weight of water.

By the hole in the lasing spectrum, we find the effective length l_{eff} of the water vapour layer corresponding to the observed transmittance $T = I_{min}/I_{max}$ for $\varphi = 2\%$ and $N = 1.2 \times 10^{16}$ cm^{-3} (Fig. 9):

$$l_{eff} = [\ln(1/T)]/(\sigma N) \approx 10^5 \text{ cm}, \qquad (3)$$

where σ is the water vapour absorption cross section.

The found l_{eff} correlates with the effective length of the absorbing layer estimated as a value proportional to the time T of stable lasing near the absorption line assuming that T is the laser spike duration ($\sim$5 μs) [12],

$$l_{eff\,T} = cT\mu \approx 10^5 \text{ cm}, \qquad (4)$$

where μ is the factor of filling the cavity with the absorbing medium.

The signal-to-noise ratio of our measuring system allowed us to reliably record the relative spectral hole depth $\Delta I/I_0 \sim 0.1$. In this case, the threshold sensitivity, i.e., the minimum absorption coefficient corresponding to the minimum recorded hole depth, can be $\sim 10^{-6}$ cm^{-1}.

In addition to the absorption inside the cavity, the laser radiation is absorbed as it propagates from the output mirror to the photodetector (through the spectrometer). Estimates show that, at a humidity of 2%, the absorption coefficient of water vapour for the path length of 1 m does not exceed 0.3%, because of which this absorption can be neglected.

6. Conclusions

The spectral characteristics of a longitudinally diode-pumped Tm:YLF laser with a selective cavity have been experimentally studied. The laser wavelength was tuned within a range of 1860–1940 nm with a linewidth not exceeding 1 nm. The effect of water vapour on the spectral characteristics of the output radiation is determined. It is shown that the Tm:YLF laser can be used for detecting water vapour in the atmosphere by intracavity laser spectroscopy.

Acknowledgements. This work was supported by the Analytical Departmental Targeted Program 'Development of the Scientific Potential of the Higher School' (Grant No. 2.1.1/3603) and by the Grant of the President of Russian Federation for Leading Scientific Schools (Grant No. NSh-2786.2008.2).

References

1. Schellhorn M. *J. Appl. Phys. B*, **91**, 71 (2008).
2. So S., Mackenzie J.I., Shepherd D.P., Clarkson W.A., Betterton J.G., Gorton E.K. *Appl. Phys. B*, **84**, 389 (2006).
3. Zakharov N.G., Antipov O.L., Savikin A.P., Sharkov V.V., Eremeikin O.N., Frolov Yu.N., Mishchenko G.M., Velikanov S.D. *Kvantovaya Elektron.*, **39** (5), 410 (2009) [*Quantum Electron.*, **39** (5), 410 (2009)].
4. Lippert E., Rustad G., Nicolas S., Arisholm G., Stenersen K. *Proc. SPIE Int. Soc. Opt. Eng.*, **5620**, 56 (2004).
5. Schellhorn M., Hirth A., Kieleck C. *Opt. Lett.*, **28**, 1933 (2003).
6. Akimov V.A., Kozlovskii V.I., Korostelin Yu.V., Landman A.I., Podmar'kov Yu.P., Frolov M.P. *Kvantovaya Elektron.*, **35** (5), 425 (2005) [*Quantum Electron.*, **35** (5), 425 (2005)].
7. Adams J.J., Bibeau C., Page R.H., Krol D.M., Furu L.H., Payne S.A. *Opt. Lett.*, **24**, 1720 (1999).
8. Sennaroglu A. et al. *Opt. Commun.*, **268**, 115 (2006).
9. Fedorov V.V. et al. *IEEE J. Quantum Electron.*, **42**, 907 (2006).
10. http://spectra.iao.ru/.
11. Bloom A.L. *J. Opt. Soc. Am.*, **64**, 447 (1974).
12. Lukyanenko S.F., Makogon M.M., Sinitsa L.N. *Vnutriresonatornaya lazernaya spectroscopiya. Osnovy methoda i primeneniya* (Intracavity Laser Spectroscopy. Principles of the Method and Applications) (Novosibirsk: Nauka, 1985).